



Synthesis, Differential Scanning Calorimetry (DSC) and Dielectric Relaxation Spectroscopy (DRS) Studies of N-methyl-N-propylpiperidinium Bis(trifluoromethylsulfonyl)imide

Boumediene Haddad ^{a,b,*}, Didier Villemin ^b, El-habib Belarbi ^a

^aDepartment of Chemistry, Synthesis and Catalysis Laboratory LSCT, Tiaret University, Tiaret, Algeria

^bLCMT, ENSICAEN, UMR 6507 CNRS, University of Caen, 6 bd Ml Juin, 14050 Caen, France

Received in 18 Sept 2011, Revised 4 Jan 2012, Accepted 4 Jan 2012.

*Corresponding author: Email: haddaboumediene@yahoo.com; Tel/Fax: +213 46 45 22 15.

Abstract

Ionic liquid based on N-methyl-N-propylpiperidinium $[MPrPPI^+]$ cation and bis(trifluoromethanesulfonyl) imide $[TFSI^-]$ anion has been synthesized and characterized. The synthesis is based on alkylation reaction of N-methylpiperidine followed by anion exchange. The structure of $[MPrPPI^+][TFSI^-]$ was identified by using 1H , ^{13}C , ^{19}F NMR and FT-IR spectroscopy. The phase behavior change for $[MPrPPI^+][TFSI^-]$ was measured in the temperature range from -150 to 200 °C by using differential scanning calorimetry (DSC). In the frequency 10^{-2} - 10^6 Hz range, dielectric measurements were performed on IL sample at various temperatures from -69 to -19 °C, i.e. around the glass transition temperature. The peak relaxation was observed near to this temperature. Also, in order to understand the ion dynamics in our IL, the frequency dependence of the complex conductivity (σ' , σ'') of $[MPrPPI^+][TFSI^-]$ at various temperatures has been analyzed. The relaxation has been characterized by the empirical Havriliak–Negami (H-N) equation.

Keywords: Ionic liquids ILs; bis(trifluoromethanesulfonyl)imide anion; Differential Scanning Calorimetry (DSC); dielectric relaxation spectroscopy (DRS); Conductivity.

1. Introduction

During the last decade, ionic liquids (ILs) have been considered as a promising green reaction media and as a novel solvent [1-4]. Initially, ILs were developed by electrochemists [5-8], who were looking for ideal electrolytes suitable for batteries [9-12]. Owing to the ionic environment effect on the chemical reactions [13-16], the main focus of electrochemists was shifted to general ionic liquid characterization in view to better applications. Ionic liquids currently have a large variety application field, which continues to expand because of their use as electrolytes for devices and processes, and solvents for organic/catalytic processes and separation/ extraction [17-20]. In addition, other applications in enzyme catalysis and multiphase bio-process operations were reported [21].

According to literature [22], the physicochemical properties of room temperature ILs consisting of *N*-alkyl-*N*-methylpiperidinium bis(trifluoro methanesulfonyl) imides have been extensively studied, in particular for their high thermal stability [23-24]. Recently, piperidinium $[TFSI^-]$ IL having a propyl and a methyl group have been prepared by many groups [25-31]. Sakaebi et al. [32,33] in their study of N-methyl-N-propylpiperidinium bis(trifluoromethanesulfonyl) imide proposed this ionic liquid as a attractive candidate for the electrolytes of Li-ion batteries with excellent safety characteristics. Which exhibited the electrochemical stability up to lithium reduction potential (<0V versus Li/Li⁺) and excellent electrochemical properties.

Since the data on dielectric properties e.g., (ϵ'), (ϵ''), ($\tan\delta$), (σ') and σ'' versus frequency, and thermal behaviour around the glass transition temperatures (T_g), of $[MPrPPI^+][TFSI^-]$ not exist in the literature. These

reason prompted us to synthesize this ionic liquid $[MPrPPI^+][TFSI^-]$, and to examine their thermal and dielectric properties.

The molecular structure of compound was characterized via 1H , ^{13}C , ^{19}F NMR and FT-IR spectroscopy, and the data of characterization are in accordance with the expected composition and structure. IL thermal properties were investigated in the temperature range from -150 to 200 °C by using differential scanning calorimetry (DSC). The frequency and temperature dependence of loss tangent ($\tan\delta$), dielectric constant (ϵ'), dielectric loss (ϵ'') and complex conductivity (σ' , σ'') is studied by using Dielectric Relaxation Spectroscopy (DRS) in the frequency range 10^{-2} - 10^6 Hz and in the temperature range from -69 to -19 °C.

2. Experimental

2.1. Reagents and materials

The reagents used in this study are: N-methyl piperidine (95 wt.%), 1-bromopropane (99.5 wt.%), Lithium bis(trifluoromethanesulfonyl) imide (LiTFSI) was obtained from 3M, diethyl ether and N,N-dimethylformamide. They were purchased from Fluka and used as received. Deionized H₂O was obtained by using a Millipore ion-exchange resin deionizer.

2.2. NMR and infrared spectroscopy measurements

1H NMR (400 MHz), ^{13}C NMR, ^{19}F (100.6 MHz) spectra were recorded on DRX 400 MHz spectrometer. The chemical shifts (δ) are given in ppm and referenced to the internal solvent signal namely TMS, and CFCl₃, respectively. IR spectra were recorded on FT-IR Perkin-Elmer Spectrum BX spectrophotometer with a resolution of 4 cm⁻¹ in the range 4000-650 cm⁻¹.

2.3.1. Synthesis of N-methyl-N-propyl piperidinium bromide $[MPrPPI^+][Br^-]$

The synthesis procedure was carried out as reported elsewhere [34]. Briefly, N-methyl piperidine and 1-bromopropane were dissolved in DMF (20 mL) before been stirred at 80 °C for 4 hours. The obtained mixture was evaporated under vacuum and washed then with diethyl ether (100 mL) to give the N-methyl-N-propyl piperidinium bromide as a yellowish solid.

2.3.2. Synthesis of N-methyl-N-propyl piperidinium Bis(trifluoromethylsulfonyl)imide

$[MPrPPI^+][TFSI^-]$ was prepared by anion exchange reaction from Br⁻ to TFSI⁻ which was carried out by mixing $[MPrPPI^+][Br^-]$ and LiTFSI (molar rate = 1:1) in water at room temperature for 2 h. The phases were separated into hydrophobic ionic liquid and aqueous phases. As described in the literature [35], the obtained $[MPrPPI^+][TFSI^-]$ was repeatedly washed with pure water to remove any starting material left in the product and then dehydrated under vacuum at 120 °C for 24 h. The structure of $[MPrPPI^+][TFSI^-]$ was confirmed by using 1H , ^{13}C , ^{19}F NMR and FT-IR spectroscopy. The details of spectrums are given below:

1H NMR (CDCl₃) δ ppm: 0.93 (t, 3H, J = 7, CH₂CH₃), 1.47-1.64 (m, 8H, 4×CH₂), 3.23-3.29 (m, 6H, 3×N⁺CH₂), 3.31 (s, 3H, N⁺CH₃); ^{13}C NMR (CDCl₃) δ ppm: 15.13, 19.51, 20.40, 24.30, 47.70, 59.63, 61.63, 123.75; ^{19}F NMR (CDCl₃) δ ppm: -78.72 (s, CF₃SO₂)₂N. IR: 2950 [ν (C-H)], 1467[δ (C-H)], 1318 [ν (S=O)], 1187 [ν (C-F)], 1140 [δ (S=O)], 1195 [δ (C-F)].

$[MPrPPI^+][TFSI^-]$ synthesized as above has the following structure:

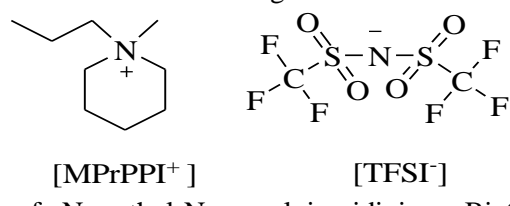


Figure 1. Chemical structure of N-methyl-N-propylpiperidinium Bis(trifluoromethyl sulfonyl) imide $[MPrPPI^+][TFSI^-]$.

2.4. Thermal analysis

Differential scanning calorimetry (DSC) thermogram was recorded by using a NETZSCH DSC 204 F1 instrument. The sample (9 mg) was placed in an aluminum pan and cooled from room temperature to -150 °C for 3 min. Subsequently, a heating scan was performed from -150 to 200 °C at a heating rate of 10 °C·min⁻¹. For this salt, a melting transition (onset temperature of the endothermic peak, T_m) and glass transition (T_g)

were observed on heating and the crystallization temperature (T_{cry}) was detected in the onset of an exothermic peak on cooling within the temperature range studied.

2.5. Measurement of dielectric properties

The dielectric measurements in the frequency range (10^2 to 10^6 Hz) and temperature interval (-69 to -19 °C) were carried out by means of a Novocontrol high resolution alpha dielectric analyzer. The analyzer was supported by Quatro temperature controller using pure nitrogen as heating agent and providing a temperature stability better than 0.2 K. Electric field in the range between 3 and 6 Vcm⁻¹ was applied. The measurements were conducted using platinum electrodes in parallel plate capacitor configuration.

For conductivity data analysis, the complex conductivity is defined as:

$$\sigma^* = \sigma' + i\sigma'' \quad (1)$$

(σ') and (σ'') are calculated from the complex permittivity as illustrated from the equations (2) and (3), respectively.

$$\sigma' = \epsilon_0 \omega \epsilon'' \quad (2)$$

$$\sigma'' = \epsilon_0 \omega \epsilon' \quad (3)$$

ϵ_0 and ω refer to the permittivity of free space and angular frequency ($\omega = 2\pi f$), respectively.

3. Results and discussion

3.1. Thermal properties

Fig. 2 show the DSC profile of [MPrPPI⁺][TFSI]. Interestingly, the glass transition was observed on heating scan by small peak at -19.7 °C, as result of a change from thermogram baseline.

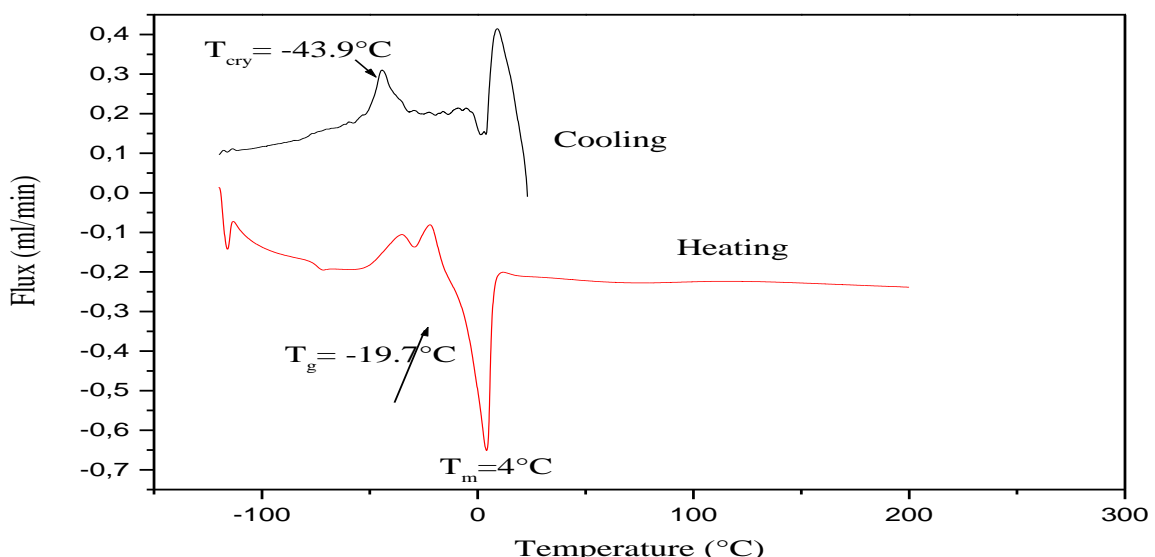


Figure 2. DSC profile of [MPrPPI⁺][TFSI].

A clear endothermic peak at 4 °C was observed, The melting point for [MPrPPI⁺][TFSI] is visibly recorded at this temperature. During cooling rang, DSC thermogram exhibit an exothermic peak which corresponds to the crystallization temperature (T_{cry}) at -43.9 °C.

Galinski et al. [36], and Salminen et al. [37] also reported that [MPrPPI⁺][TFSI] exhibited a T_m at -8.7 and 9 °C respectively, in a series of papers. They emphasized the importance of the difference in the residual water content and measuring condition etc.

3.2. Dielectric analysis

The complex permittivity can be expressed as a complex number:

$$\epsilon^*(\omega) = \epsilon'(\omega) - i\epsilon''(\omega) \quad (4)$$

The real part $\epsilon'(\omega)$ and imaginary one $\epsilon''(\omega)$ of the complex permittivity spectra are determined. Consequently, the loss factor is calculated as follows:

$$\tan(\delta(\omega)) = \epsilon''(\omega) / \epsilon'(\omega) \quad (5)$$

With respect to the different temperatures, the relaxation time, τ , is calculated according to the resonance condition which is defined by $\omega\tau=1$ from the peak maximum of $\tan(\delta(\omega))$.

3.2.1. The frequency and temperature dependence of (ϵ') and (ϵ'')

In Fig. 3 (a and b), the real and imaginary parts of the complex permittivity of $[\text{MPrPPI}^+][\text{TFSI}]$ as a function of frequency at various temperatures are presented.

For the data analysis, we observe that the ϵ'' and ϵ' , reduces with the temperature and the frequency increasing, converging to a constant value, ϵ'_∞ and ϵ''_∞ , respectively, whatever applied temperature.

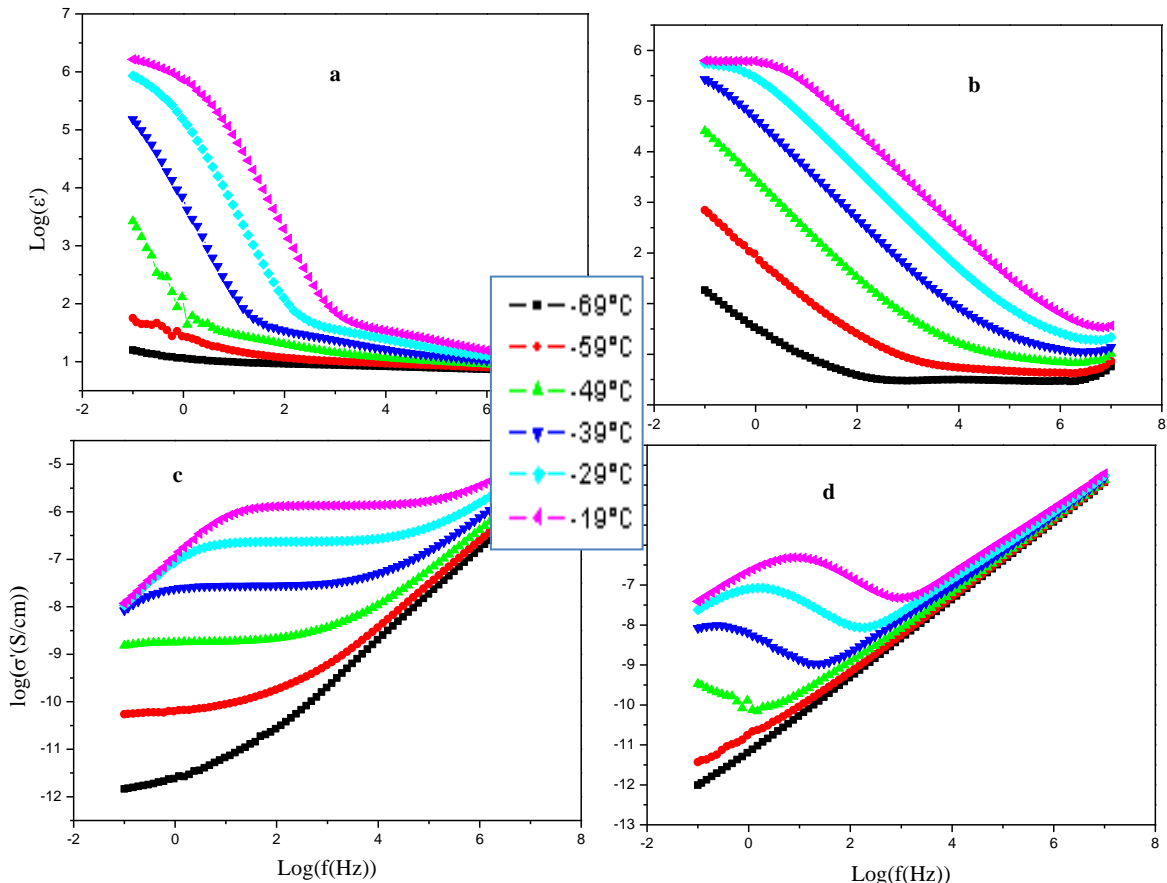


Figure 3. Complex dielectric function ($\epsilon^*(\omega) = \epsilon'(\omega) - i\epsilon''(\omega)$) and complex conductivity function ($\sigma^*(\omega) = \sigma'(\omega) + i\sigma''(\omega)$) of $[\text{MPrPPI}^+][\text{TFSI}]$ at different temperatures.

It was shown that

- In the frequency range between 10 to 10^3 Hz, the permittivity of $[\text{MPrPPI}^+][\text{TFSI}]$ decreases rapidly with the increasing frequency, especially in the temperature range from -19 to -49 °C. The contribution of this part is attributed to the mobile ions which near glass transition temperature, T_g , i.e. roughly -19.7 °C.

- A constant value (ϵ_∞) was obtained at a frequency higher than 10⁶ Hz. However, the permittivity of [MPrPPI⁺][TFSI] decreases slightly with the increasing frequency for temperature range studied and in the frequency range between 10³ to 10⁶ Hz, the contribution of this part is due to the localized charge carrier in our IL.

3.2.2. The frequency and temperature dependence of (σ') and (σ'')

The conductivity is one of the most important properties of ILs as electrolyte materials, the frequency dependence of the complex conductivity (σ' , σ'') of [MPrPPI⁺][TFSI] at various temperatures are shown in Fig. 3 (c and d).

The conductivity σ' is characterized on the low frequency side by the plateau the value of which directly yields the *dc* conductivity, σ_0 , and the characteristic radial frequency, ω_c ($\omega=2\pi f$), at which dispersion sets in and turns into a power law at higher frequencies. Systematically varying the temperature while keeping the same frequency range results in significant differences in the charge transport quantities (i.e., σ_0 varies from T= -69 to -19 °C over 4 decades). With an increase in temperature, the conductivity increases.

It indicated that the linear variation of the imaginary part of conductivity σ'' with frequency was observed at the frequency range from 10³ to 10⁶ for several temperatures.

On the other hand, the real part of the dielectric function ϵ' at $f_c = (\omega_c/2\pi)$ turns from the high frequency limit to the static value ϵ_s . At lower frequencies, it is observed that σ' decreases from σ_0 and this is due to electrode polarization that results from blocking of charge carriers at the electrodes.

Krause et al. [38], and Min et al. [39], also reported the similar trend in conductivity of various ILs in a series of papers. They demonstrated that the peaking of σ'' spectra in the low frequency region manifests the electrode polarization and the spectral range in the strong temperature dependence of the charge transport processes.

3.2.3. The frequency and temperature dependence of ($\tan\delta$)

Fig.4 show the dielectric spectra in terms of the loss factor $\tan\delta = \epsilon''/\epsilon'$ versus the frequency for [MPrPPI⁺][TFSI]. We noticed clearly that the loss tangent parameter has a same shape and similar values around ($\tan\delta = 39$) with a same symmetric degree from -69 to -29 °C range temperature.

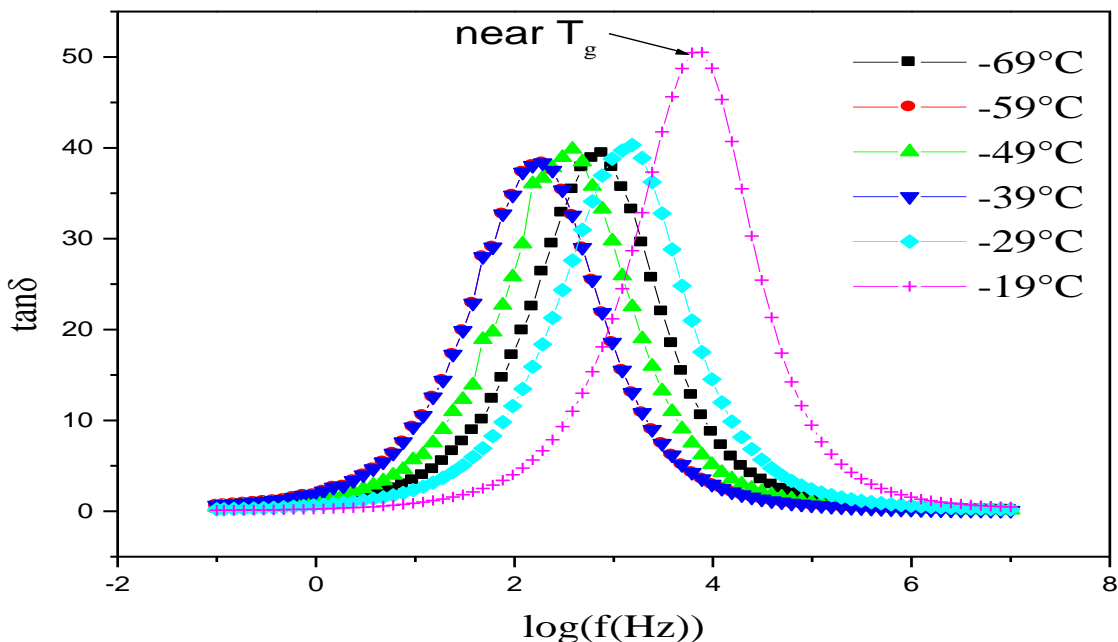


Figure 4. Frequency dependence of the loss factor $\tan\delta$ measured at different temperatures of [MPrPPI⁺][TFSI].

Moreover, we observed a maximum value of loss factor ($\tan\delta = 50$) near the glass transition temperature, T_g , i.e. roughly 19.7 °C (Fig 4). Near this temperature, the mobility of the ions is quite high, the result is that the polarisability suddenly increases at T_g resulting a peak on $\tan\delta$ as Frequency, which has been described elsewhere and reported in previous studies [40-43] that the dielectric T_g originates from the reorientation of molecules.

The dielectric spectra of the relaxations were fitted using the empirical Havriliak-Negami (HN) function expressed as:

$$\varepsilon_{HN}^* = \varepsilon_\infty + \frac{\Delta\varepsilon}{[1 + (i\omega\tau_{HN})^\beta]^\gamma} \quad (6)$$

where $\Delta\varepsilon$ is the dielectric strength, ε_∞ is the relaxed value of ε' , τ_{HN} is the Havriliak-Negami relaxation time (related to the relaxation time), β and γ are shape parameters.

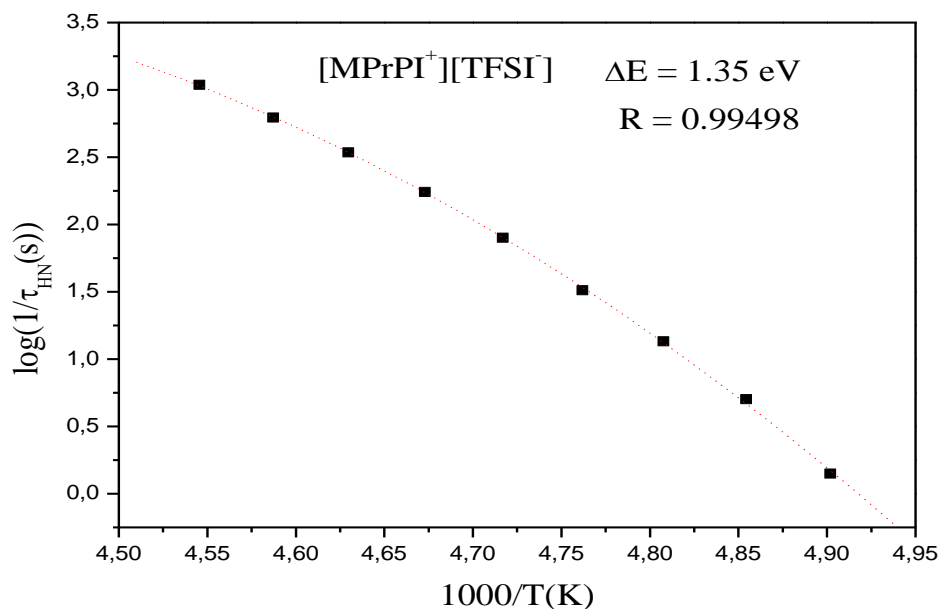


Figure 5. Temperature dependence of the relaxation times: activation plot of logarithm $\ln(1/\tau_{HN})$ vs. reciprocal of temperature $1/T$: (R) Correlation coefficient.

As shown in the Fig.5, the temperature dependence of the relaxation time can be modeled by a Vogel-Fulcher-Tammann equation. This dependence can be described by (eq.7),

$$\tau(T) = \tau_0 \exp\left[-\frac{E_A}{K_B(T - T_0)}\right] \quad (7)$$

Where, T_0 is the Vogel-temperature (sometimes referred to as the ideal glass transition temperature), τ is relaxation time, τ_0 is relaxation time pre-exponential factor, and k_B is Boltzmann constant.

The activation energy of $[MPrPPI^+][TFSI^-]$ was found to be 1.35 eV for the relaxation process. This value is in good agreement with other values previously published in the literature for relaxation process in different series of imidazolium based ionic liquids.

Conclusion

In this work, N-methyl-N-propylpiperidinium Bis(trifluoromethylsulfonyl)imide was prepared from *N*-methylpiperidine in two steps and its thermal properties and dielectric relaxation properties were studied. ¹H, ¹³C, ¹⁹F NMR and FT-IR spectroscopy were applied to identify the molecular structure of compound.

Results of DSC studies indicate the presence of three phases: (T_g) at -19.7, (T_m) at 4 and (T_{cry}) at -43.9 °C during the programmed (heating–cooling) steps.

The maximum value of the loss factor is observed for the [MPrPPI⁺][TFSI] near to glass transition temperature, T_g . The dielectric permitivity, $\epsilon'(\omega)$ and its variations with frequency and temperature, indicate a dispersion at frequency lower than 1 kHz, due to the increase in electrode polarization. The dielectric loss ϵ'' decrease on increasing the frequency, this can be explained by means of the dielectric polarization mechanism of our Ionic liquid.

The conductivity varied from 9.3×10^{-13} S/cm at -69 °C to 2.3×10^{-8} S/cm at the temperature near to glass transition temperature, T_g . The activation energy of [MPrPPI⁺][TFSI] was found to be 1.35 eV for the relaxation process.

Acknowledgement

We gratefully acknowledge the program national exceptional (PNE -Algeria) for its financial support. The authors thank professor Kremer from Institute of Experimental Physics I, University of Leipzig for the dielectric measurements of the ionic liquids.

References

1. Rogers, R.D., Voth, G.A., *Acc. Chem. Res.*, 40 (2007) 1077-1078.
2. Wasserscheid, P., Welton T., *Ionic Liquids in Synthesis*, Second ed. Wiley-VCH, Verlag, Weinheim, (2003).
3. Wilkes, J.S., *Green Chem.*, 4 (2002) 73-80.
4. Rogers, R.D., Seddon, K.R., (Eds.), *Ionic Liquids: Industrial Applications to Green Chemistry*, ACS Symposium Series, vol. 818, American Chemical Society, Washington, DC, (2002).
5. Ohno H., (Ed.), *Electrochemical Aspects of Ionic Liquids*, Wiley-Interscience, Hoboken, New Jersey (Chapter 4), (2005).
6. Appetecchi, G.B., Montanino, M., Zane, D., Carewska, M., Alessandrini, F., Passerini, S., *Electrochim. Acta*, 54 (2009) 1325-1332.
7. MacFarlane, D.R., Forsyth, M., Howlett, P.C., Pringle, J.M., Sun, J., Annat, G., Neil, W., Izgorodina, E.I., *Acc. Chem. Res.*, 40 (2007) 1165-1173.
8. Galinski, M., Lewandowski, A., Stepniak, I., *Electrochim. Acta*, 51 (2006) 5567-5580.
9. Sun, X.G., Dai, S., *Electrochim. Acta*, 55, (2010) 4618-4626.
10. Balakrishnan, P.G., Ramesh, R., Prem Kumar, T., *J. Power Sources*, 155 (2006) 401-414.
11. Wu, T.Y., Su, S.G., Gung, S.T., Lin, M.W., Lin, Y.C., Lai, C.A., Sun, I.W., *Electrochim. Acta*, 55 (2010) 4475-4482.
12. Matsumoto, H., Sakaebe, H., Tatsumi, K., *J. Power Sources*, 146 (2005) 45-50.
13. Haumann, M., Riisager, A., *Chem. Rev.*, 108 (2008) 1474-1497.
14. Olivier-Bourbigou, H., Magna, L., *J. Mol. Catal. A: Chem.*, 182 (2002) 419- 437.
15. Martins, M.A.P., Frizzo, C.P., Moreira, D.N., Zanatta, N., Bonacorso, H.G., *Chem. Rev.*, 108 (2008) 2015-2050.
16. Fraga-Dubreuil, J., Bourahla, K., Rahmouni, M., Bazureau, J.P., Hamelim, J., *J. Catal. Commun.*, 3 (2002) 185-190.
17. Han, X., Armstrong, D.W., *Acc. Chem. Res.*, 40, (2007) 1079-1086.
18. Visser, A.E., Swatloski, R.P., Reichert, W.M., Mayton, R., Sheff, S., Wierzbicki, A., Davis, J.H., Rogers, R.D., *Environ. Sci. Technol.*, 36, (2002) 2523-2529.
19. Huddleston, J.G., Willauer, H.D., Swatloski, R.P., Visser, A.E., Rogers, R.D., *Chem. Commun.*, (1998) 1765-1766.
20. Liu, S., Xiao, J., *J. Mol. Catal. A: Chem.*, 270 (2007) 1-43.
21. Yim, T., Lee, H.Y., Kim, H.-J., Mun, J., Kim, S., Oh, S.M., Kim, Y.G., *Bull. Korean Chem. Soc.* 28, (2007) 1567-1572.

22. Lewandowski, A., Swiderska-Mocek, A., *J Appl Electrochem*, 40 (2010) 515–524.
23. Sun, X.G., Dai, S., *Electrochim. Acta*, 55 (2010) 4618-4626.
24. Sun J., MacFarlane .D.R., Forsyth M., *Ionics*, 3 (1997) 356-362.
25. Galinski, M., Lewandowski, A., Stepiak, I., *Electrochimica Acta*, 51 (2006) 5567–5580.
26. Ogiara W., Washiro S., Nakajima H., Ohno H., *Electrochimica Acta*, 51 (2006) 2614–2619.
27. MacFarlane, D. R.; Meakin, P.; Sun, J.; Amini, N.; Forsyth, M, *J. Phys. Chem. B*, 103 (1999) 4164-4170.
28. McFarlane, D. R.; Sun, J.; Golding, J.;Meakin, P.; Forsyth, M, *Electrochimica Acta*, 45 (2000) 1271-1278.
29. Barisci, J. N.; Wallace, G. G.; MacFarlane, D. R.;Baughman, R. H. *Electrochem. Commun*, 6 (2004) 22-27.
30. Howlett, P. C.; Brack, N.; Hollenkamp, A. F.; Forsyth, M.; MacFarlane, D. R, *J. Electrochem. Soc*, 153 (2006) 595-606.
31. Matsumoto, H.; Sakaeb, H.; Tatsumi, K., *J. Power Sources*, 146 (2005) 45-50.
32. Sakaeb, H.; Matsumoto, H.; Tatsumi, K., *Electrochimica Acta*, 53 (2007) 1048–1054.
33. Sakaeb, H., Matsumoto, H., *Electrochem. Commun*, 5 (2003) 594-598.
34. Min, G.-H., Yim, T., Lee, H.Y., Kim, H.-J., Mun, J., Kim, S., Oh, S.M., Kim, Y.G., *Bull. Korean Chem. Soc*, 28 (2007) 1562-1566.
35. Xiang H.F., Yin B., Wang H., Lin H.W., Ge X.W., Xie S., Chen C.H., *Electrochimica Acta*, 55 (2010) 5204–5209.
36. Galinski, M., Lewandowski, A., Stepiak, I., *Electrochim. Acta*, 51 (2006) 5567-5580.
37. Salminen, J., Papaiconomou, N., Kumar, R.A., Lee, J.M., Kerr, J., Newman, J., Prausnitz, J.M., *Fluid Phase Equilib*, 261 (2007) 421–426.
38. Min Y.J., Akbulut M., Sangoro J.R., Kremer F., Israelachvili J., *J. Phys. Chem. C*, 113 (2009) 16445–16449.
39. Krause, C., Sangoro, J.R., Iacob, C., Kremer, F., *J. Phys. Chem. B*, 114 (2010) 382–386.
40. Adachi, K., Hirano, H., *Macromolecules*, 31 (1998) 3958-3962.
41. Goitiandia, L., Alegria, A., *J. Chem. Phys*, 121 (2004) 1636-1643.
42. Pradhan, N. R., Iannacchione, G. S., *J. Appl. Phys*, 43 (2010) 1-7.
43. Haddad, B., Villemin, D., Belarbi, E-H., Bar, N., Rahmouni, M., *Arabian Journal of Chemistry*, (doi:10.1016/j.arabjc.2011.01.002), (2011) in press.

(2012) <http://www.jmaterenvironsci.com>